Materials and Design 196 (2020) 109160

Contents lists available at ScienceDirect

Materials and Design

journal homepage: www.elsevier.com/locate/matdes

$Li_4Br(OH)_3$ microstructure monitoring over its synthesis to tackle the lithium-based salts exploitation challenges as advanced phase change materials for storage technologies

P. Legros [a], E. Lebraud [b], M. Duquesne [c], F. Achchaq [d,*]

[a] PLACAMAT, UMS 3626, 87 Avenue du Docteur Schweitzer, 33608 Pessac Cedex, France
[b] ICMCB UMR CNRS 5026, 87 Avenue du Docteur Schweitzer, 33608 Pessac Cedex, France
[c] Bordeaux INP, University of Bordeaux, CNRS, Arts et Metiers Institute of Technology, INRAE, I2M Bordeaux, F-33400 Talence, France
[d] University of Bordeaux, CNRS, Arts et Metiers Institute of Technology, Bordeaux INP, INRAE, I2M Bordeaux, F-33400 Talence, France

HIGHLIGHTS

- An inorganic Li-salts study to foster the further design of sensible and latent thermal energy storage units is presented.
- Highlighting of the LiOH distorted lattice, before melting, impacting its reaction with LiBr.
- Advanced phase change material: $Li_4Br(OH)_3$ in situ/real time observations, charted in the current LiOH/LiBr phase diagram.
- Highlighting of two $Li_4Br(OH)_3$ structures, each with its own final macroscopic properties.
- LiOH decomposition impact on the attempt of $Li_4Br(OH)_3$ formation: deviation towards a new phase.

GRAPHICAL ABSTRACT

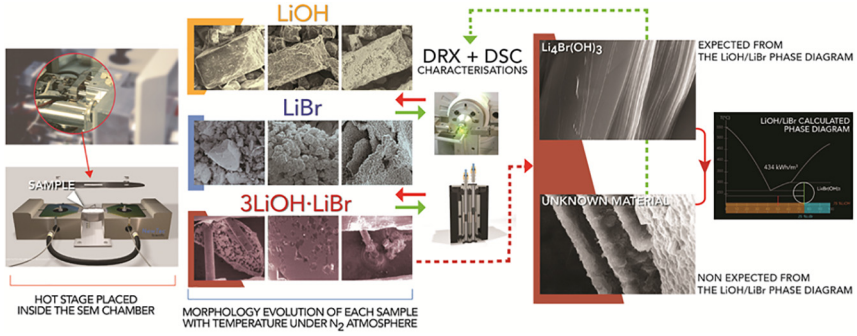

ARTICLE INFO

Article history:
Received 30 June 2020
Received in revised form 14 September 2020
Accepted 15 September 2020
Available online 18 September 2020

Keywords:
Energy-storage
Heat energy
Lithium salts
Mechanism synthesis
Microstructure characterisation
Microstructure observation

ABSTRACT

How to overcome fastly and reliably the challenges to foster the lithium-based salts exploitation for latent heat storage technologies? *In situ* and real time microscopy is used to understand the discrepancies between the theoretical and experimental macroscopic properties of materials *via* the microscopic mechanisms. The feasibility of this method on the inorganic lithium salts is demonstrated despite their air/moisture-sensitivity and the common belief pretending that LiOH cannot be used for the synthesis of new materials inside the microscope chamber due to its decomposition in dry environment or under vacuum. The deviation source of ~30% from the theoretical energy density of 434 kWh/m^3 has been investigated through the case study of $Li_4Br(OH)_3$, an uncommon promising phase change material. The hydration/dehydration of the starting materials appears as one of the main parameters, with applied temperature protocols, eliciting the deviation towards different materials from the targeted one of interest, in terms of morphology and properties. This criterion, if not taken into account, could be disastrous for the storage capacity of a unit during its use. This study highlights solutions to avoid these deficiencies. The results consistency at microscale with those obtained at macroscale is also proved despite the different operating conditions

* Corresponding author.
E-mail address: fouzia.achchaq@u-bordeaux.fr (F. Achchaq).

https://doi.org/10.1016/j.matdes.2020.109160

1. Introduction

As recently recognised, the lithium compounds are now also considered as an alternative for the development of thermal energy storage materials. They are particularly investigated as Phase Change Materials for the Latent Heat Storage technologies in order to allow a simple use of renewable energies. These materials could for instance be integrated in the storage units of the solar power applications or any other standard power plants providing direct steam generation around 300 °C. However, their drawbacks, such as moisture-sensitivity, decomposition, corrosiveness, low thermal stability…, brake their studies in depth and in use. Theory shows us the possibility to find suitable materials with outstanding and appropriate properties but their experimental development remains a challenge for researchers and engineers in materials science [1,2]. This work focuses on how overcome fastly and reliably these drawbacks to foster this emergent topic of research for LHS. To this purpose, $Li_4Br(OH)_3$ has been theoretically and experimentally identified as a very promising thermal energy storage material. *De facto*, $Li_4Br(OH)_3$ could be used in ultra-compact storage units for the applications with a working temperature around 300 °C. However, despite the successful $Li_4Br(OH)_3$ synthesis at macroscale, there are still several missings. Its morphology remains unknown and the preliminary thermal analysis performed to access to its thermodynamic properties indicates that a deeper understanding of the involved synthesis mechanisms is required. Despite the very interesting enthalpy value of ~570 kJ/kg obtained during the first experiments, it still remains far from the 800 kJ/kg value predicted by the theory [3]. The $Li_4Br(OH)_3$ formation investigation at microscale allows the knowledge deepening of the phase transition mechanisms occurring during the synthesis and leading to the properties of the targeted end material at macroscale. This investigation should help (i) to determine the right temperature protocol to be used at macroscale in order to systematically obtain the targeted end product, (ii) to understand why this deviation of ~30% has been observed, (iii) to verify a potential link between the high moisture-sensitivity of the raw materials and the obtained end product: according to the LiOH/LiBr phase diagram, the $Li_4Br(OH)_3$ peritectic compound exists only if the starting materials are completely anhydrous. Yet, the lithium compounds are known to react rapidly and continuously with water available in air if exposed to air with a relative humidity greater than 15%, leading hence to their oxidation [4,5] and, (iv) to determine the best working conditions in a faster way to avoid the problems encountered at macroscale (leakage, chemical incompability between the heat storage material and its container…). In materials science, these points led to the development of sophisticated experimental techniques to associate both *in situ* characterisation and imaging results. In this way, the knowledge about the mechanisms underlying the solidification microstructures following a liquid-solid transition has been significantly deepened by using the directional solidification technique (DS), infrared thermography (IRT) or confocal scanning laser microscopy (CSLM) [6–10]. The use of environmental scanning electron microscopes (SEM) coupled with specific devices to perform *in situ* and real time experiments is another complementary method allowing direct studies at microscale of the materials under constraints (mechanical, wetting, thermal…) [11,12]. In this work, the reaction mechanisms involved in the $Li_4Br(OH)_3$ synthesis has been studied by using a SEM coupled with a hot stage focusing on the starting materials transformation processes first [13–19]. One of the major advantages of this technique is the rapid, direct, *in situ* and real time observations of the thermally-induced transitions, including the solid/liquid one. The impact of the reversible LiOH decomposition into Li_2O on the $Li_4Br(OH)_3$ synthesis has been examined, as it has been done to clarify its role in the ionic conductivity of Li_5AlO_4 [385–450 °C] [13] or in order to be used as a phase change material to damp the exhaust temperature vibrations of cars for instance [15]. The studies on LiBr are mainly dealing with its solubility and crystallisation in aqueous solutions in order to be used as a sorbent for heat storage [16,17]. There are a very few works about the anhydrous LiBr behaviour in literature such as those of [18,19] reporting the effects of LiBr on the calcium oxide powders decomposition or, the use of anhydrous LiBr to develop a new family of Li-rich anti-perovskites for electrochemical batteries. Hitherto, no similar work to that the following one, dedicated to the thermally-induced transitions of LiOH and LiBr inside a HT-SEM, has been reported. This lack is likely due to the corrosiveness and to the hazard profile of the inorganic anhydrous salts that braked their study as well to the "black-box" aspect of all complementary techniques commonly used and the phenomena's scale to be studied. This work provides the details of the LiOH decomposition process upon heating. The LiOH intermediate surface formed during this step is thus observed for the first time to the best of our knowledge [20]. The critical links between the processing conditions, the microstructure formation and the targeted end product have been highlighted and compared with the theoretical steps of the current calculated LiOH/LiBr phase diagram [3,21]. The understanding of the transport mechanisms through LiOH and LiBr facilitates that of the reaction mechanisms during the $Li_4Br(OH)_3$ synthesis process. This kind of material would require the design of a single tank passive latent storage unit with a heat transfer fluid in direct contact working at ambient pressure. The reversible solid-liquid transition would occur inside this tank avoiding the major difficulty, related to the solidification phenomenon, encountered usually in the sensible heat storage systems using the molten salts. LiOH and LiBr intervening in most of binary and multicomponents lithium-based candidates for LHS, these results represent also the first step to facilitate the development of the other lithium-based candidates as well their mechanisms understanding.

2. Experimental section

2.1. Materials and characterisation methods

The sample preparation takes place inside an argon controlled atmosphere glove box to avoid oxidation or hydration of LiOH, LiBr and of the studied mixtures. The 3LiOH·LiBr peritectic composition is made up of LiOH and LiBr powders supplied by Acros Organics with a purity of, respectively 99+ % and 98% and with LiOH and LiBr powders, supplied by Alfa Aesar, with a purity of 99.995% for both of them. The calculations show that the impurities presence is so weak (<<1%) for the Acros Organics chemicals that this cannot impact on the $Li_4Br(OH)_3$ formation and indeed, $Li_4Br(OH)_3$ has been synthesized whatever the used starting materials. The XRD diffractograms show however that there is the presence of a few water molecules in the educts of Acros Organics whereas those of Alfa Aesar are completely anhydrous. Knowing that LiOH decomposes into Li_2O under vacuum or dry atmospheres upon heating and that this decomposition is reversible [20,22–24], Li_2O and LiBr (slightly hydrated, Acros Organics) are also be used as non anhydrous starting materials to form the $3Li_2O·2LiBr$ mixture in order to verify that a certain amount of $Li_4Br(OH)_3$ can be directly produced without using LiOH. The samples are either placed inside sealed glass tubes as powdery or they are first cold pressed into pellets to enhance the grains contact as well as the contact with the crucible bottom of the hot stage during the heating treatment. Each piece of a pellet of 1.0 ± 0.2 mm of thickness is kept in its dried glass tube. The samples are then heated and cooled inside a stainless steel crucible of the hot stage (supplier: NewTec scientific, Fig. 1) placed inside the environmental scanning electron microscope chamber (SEM; Zeiss 50 Evo). The stainless steel protection is used to avoid the consequences of the explosive generation of steam occurring sometimes due to the bulk water "carry-over" in LiOH. This protection allows also minimising the temperature gradient inside the crucible. The experiments are performed at secondary vacuum (10^{-4} Pa) and then, at nitrogen-rich environment of different partial pressures. The results being the same, the value is then fixed arbitrarily at 10 Pa.

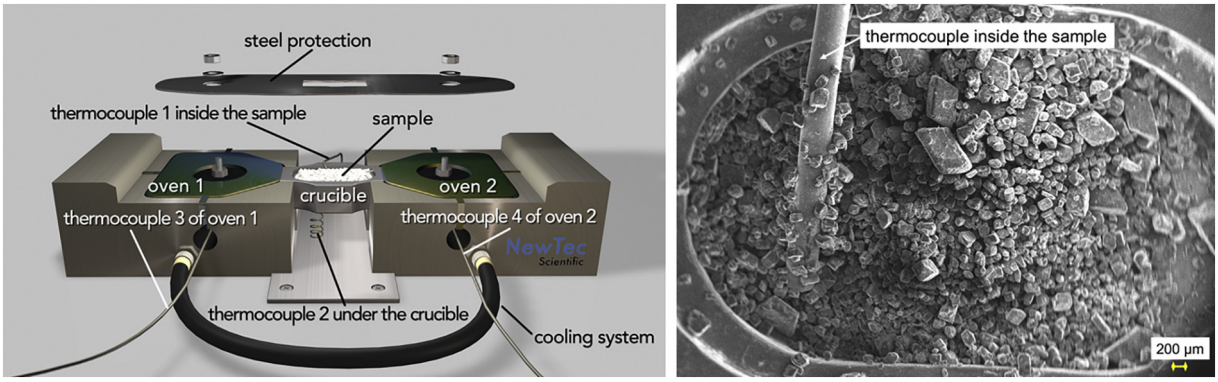

Fig. 1. On the left, the hot stage used for the HT-SEM experiments made up of two ovens allowing applying either a homogeneous working temperature or a temperature gradient. A protection is added to avoid, as possible, the heat loss and the SEM chamber contamination, without avoiding the sample visual monitoring. On the right, top view of LiOH powder inside the HT-SEM stainless steel crucible.

At the end of each experiment, a few droplets of inert mineral oil is deposited on the sample. This protects it from the atmosphere the required time to put it in the XRD holder and to analyse it (PANALYTICAL X'PERT 3 Powder diffractometer; MoK α radiation (λ = 0.71073 Å)). The $Li_4Br(OH)_3$ morphology is recognised after its XRD signature has been compared with that obtained by using the protocol described in [3].

Regarding the LiOH and LiBr studies, the sample of 50 mg is placed inside the calibrated DSC furnace (Sensys 3D; SETARAM) with a dry argon flow at 30 mL/min to ensure that the crucible remains in an inert atmosphere. The maximum value of the applied program temperature corresponds to 20 °C above the melting temperature of each starting material. The first temperature program, repeated several times, is as follows: (i) from ambient temperature to the maximum temperature at a scanning rate of 0.3 °C/s; (ii) maintaining the maximum temperature for 5 min; and (iii) decreasing to ambient temperature at the scanning rate of 0.1 °C/s. This temperature program is followed by a second one, repeated also several times: (i) from ambient temperature to the maximum temperature at a scanning rate of 0.1 °C/s; (ii) maintaining the maximum temperature for 5 min; and (iii) decreasing to ambient temperature at the scanning rate of 0.01 °C/s. The DSC measurements have been repeated in triplicate for each sample.

Regarding the 3LiOH·LiBr and $3Li_2O·2LiBr$ mixtures, the same first temperature program as that for the starting materials is applied due to the LiOH behaviour (see subsection 3.1.3.).

2.2. Heat treatment protocols used for the SEM hot stage

A tin-lead eutectic has been used as reference material to confirm the temperature acquisition reliability. The temperature acquisition is performed by using a type K thermocouple placed under, and in contact with, the crucible (precision = 1 °C). The same heat treatment is applied to the reference material at secondary vacuum (10^{-4} Pa), at a constant pressure of 10 Pa and at the atmospheric one. Supplementary videos 1a/ and 1b/ show an example of the reference material melting at

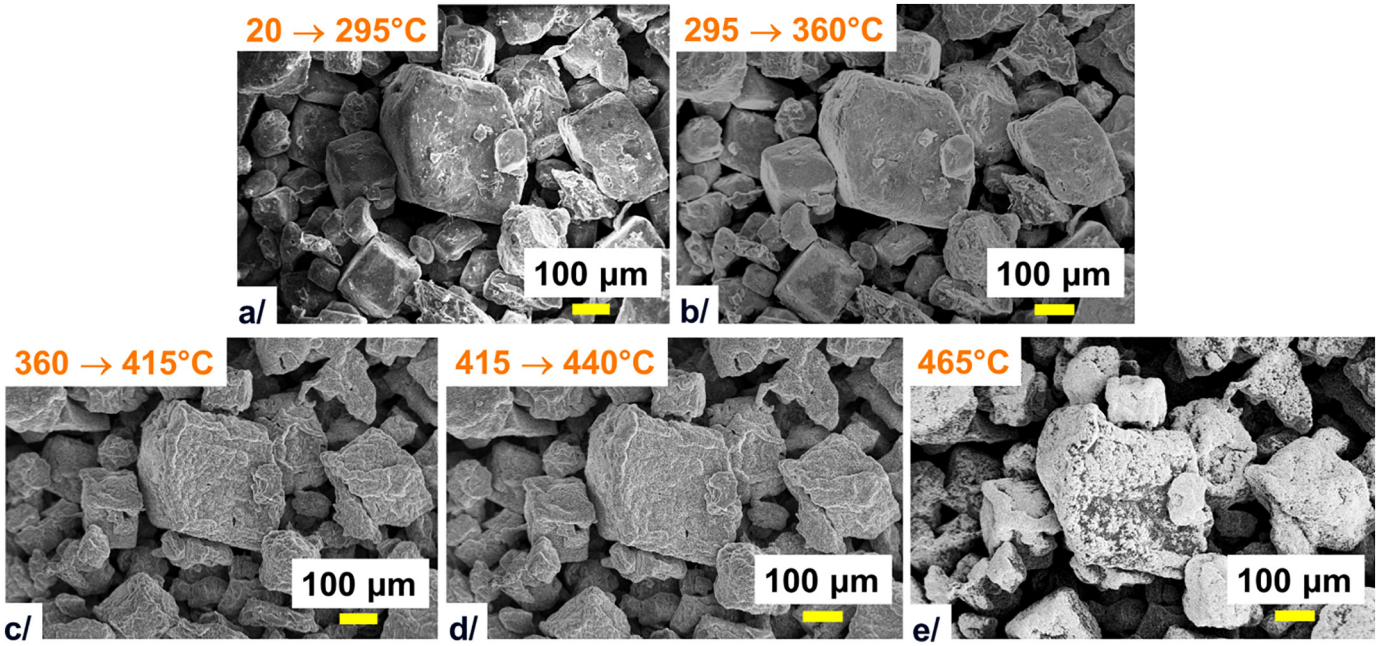

Fig. 2. a/ Thermally-induced transitions of LiOH powder during the heating step under secondary vacuum with b/—d/ a highlight of the intermediate surface of LiOH, and e/ at the beginning of the surface conversion into Li_2O.

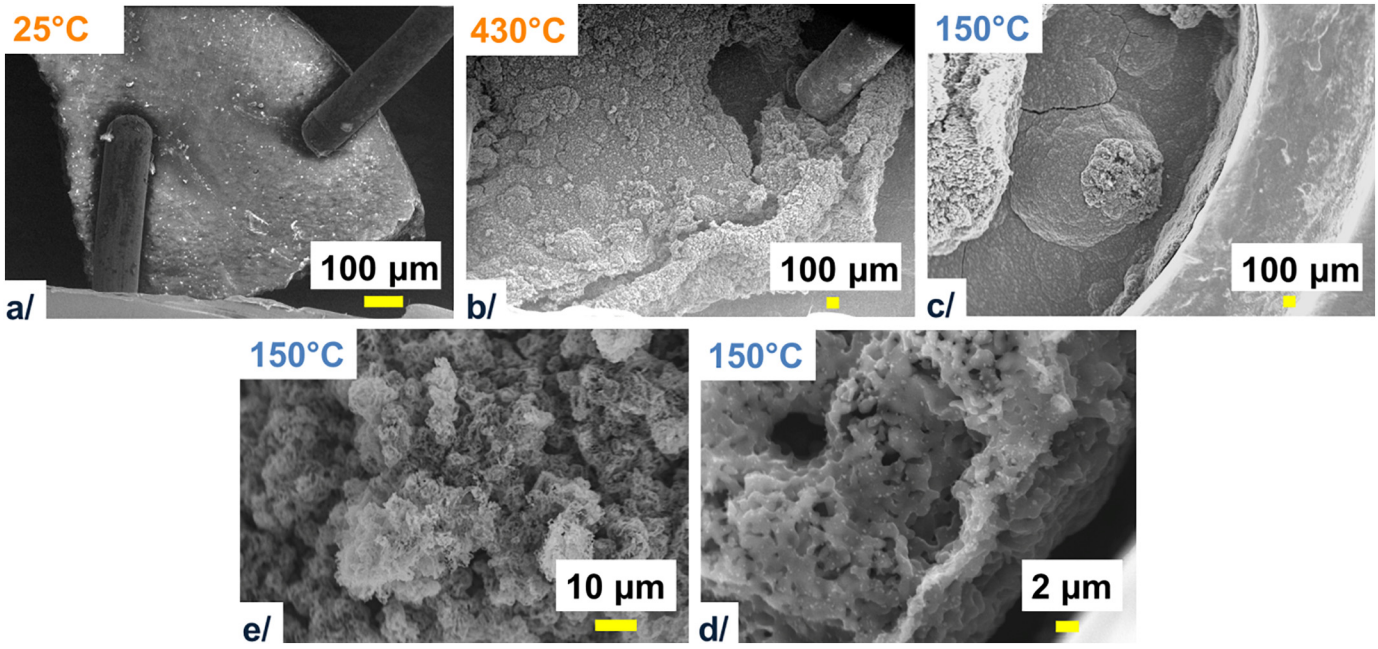

Fig. 3. a/—c/ Highlight on the LiOH melting during the heating step and after cooling at a partial pressure of 10 Pa. e/—d/ Zoom in on the sample at the edge of the crucible.

secondary vacuum and at 10 Pa. The recorded melting temperature is in well agreement with the value obtained at the atmospheric pressure and mentioned in literature (183 ± 1 °C). The recorded temperatures by using the thermocouple sheathed with inconel in direct contact with the sample are not reliable due to the materials' behaviours (see subsection 3.1.4.). Hence, all the following mentioned values are those recorded by the thermocouple placed under and in contact with the crucible bottom, as in a DSC device. Then, a series of heat treatment experiments are performed *in situ* and real time on a few mg of LiOH, LiBr, powdery mixtures and cold-pressed pellet samples. All measurements are first carried out in the temperature range of 25–700 °C at secondary vacuum, and then, at 10 Pa to determine the working temperature ranges of interest of each studied composition. The appropriate heating/cooling scanning rates have been determined after several tests. The chosen values, that will be also used for the thermophysical characterisations in further tougher studies (DSC), allow focusing on the occurring mechanisms. The applied heating scanning rate is then of 0.4 °C/s from room temperature up to 20 °C below the minimum temperature value of the interval of interest and of 0.1 °C/s up to the material's melting temperature experimentally defined. The cooling scanning rate is fixed at 0.1 °C/s. Some phenomena have occurred so fast during heating or cooling that the temperature has been hold the required time to take a picture.

3. Results and discussion

3.1. LiOH and LiBr phase transitions

3.1.1. LiOH under vacuum condition

The evolution of powdery LiOH (purity: 99.995%) with temperature during the heating step under secondary vacuum is illustrated in Fig. 2. LiOH grains transform very slightly from room temperature

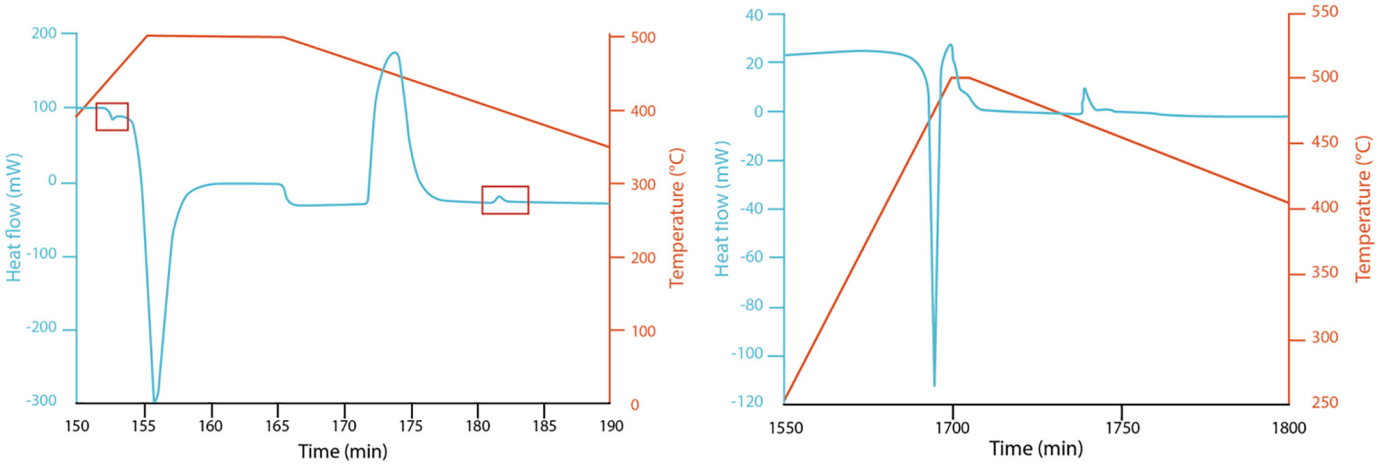

Fig. 4. LiOH underwent 6 thermal cycles: Here on the left, third LiOH thermogram obtained at a heating scanning rate of 0.3 °C/s. The red frames show the LiOH softening. On the right, the third thermogram obtained for a heating scanning rate of 0.1 °C/s. The same palier of 5 min at 500 °C has been applied for both protocols. (For interpretation of the references to colour in this figure legend, the reader is referred to the web version of this article.)

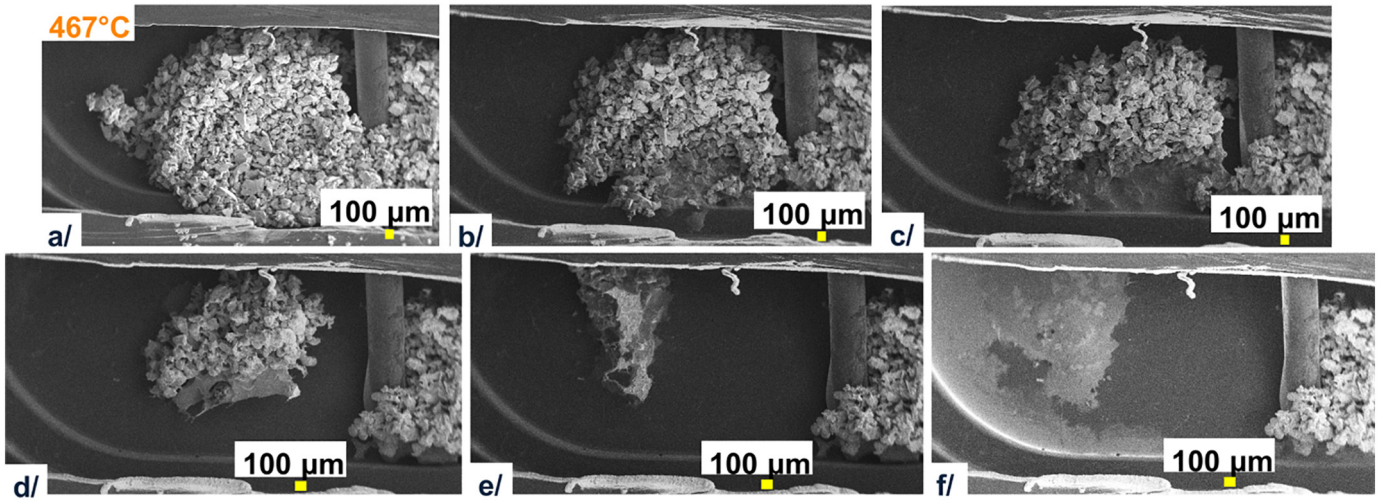

Fig. 5. Thermally-induced transitions of ground LiBr under secondary vacuum during the heating step maintained at 467 °C.

up to ~360 ± 1 °C. The transformation, with a clear and uneven bloating phenomenon on the edges of the grains first, moves inward from the surface. This occurs together with an increase of the porosity at ~415 ± 1 °C. A slight grains expansion can also be observed up to ~440 ± 1 °C. Another transformation takes place at their surface at ~440 ± 1 °C as a solid state white blanket due to the LiOH decomposition, that presents a flaky morphology when the temperature reaches ~550 ± 1 °C (see supplementary Fig. 1). Then, no further significant change is observed even when the temperature value reached 715 °C. Surprisingly, no melting of LiOH has been observed whereas its reported melting temperature is of 462 ± 5 °C – 471 °C at ambient pressure [14,24]. No further significant transformation has been observed during the cooling step up to the room temperature afterwards (see supplementary Fig. 2).

These *in situ* and real time observations show all the LiOH decomposition process steps proposed by [24] in their theoretical model by providing finer details on the evolutionary behaviour of the grains. Dinh et al. assumed that LiOH, of micrometer grain sizes, decomposes through a phase boundary motion, moving inward from the surface with a rate limiting mechanism leading to four steps: (i) vacuum (or extreme dry environment)/LiOH interface converts into an intermediate surface of LiOH with a distorded lattice that facilitate its decomposition, (ii) this intermediate surface converts then into Li_2O due to the surface bond weakness with the water release, (iii) creation of another intermediate surface trapped between the previous formed Li_2O layer and the remaining LiOH core and finally, (iv) the LiOH core conversion into Li_2O.

This process, once triggered, goes on even if heating is stopped but, on the one hand, this can be controlled and, on the other hand, this is a reversible phenomenon as also shown by [24].

3.1.2. LiOH under low pressure condition

Fig. 3 shows the evolution of the LiOH pellet (purity: 99.995%) with temperature during the heating step and at 150 °C during the cooling step under nitrogen-rich environment at 10 Pa. The same phenomena, as described in subsection 3.1.1 in terms of bloating, increasing porosity and transformation from the surface to the core are observed but with, this time, the highlighting of the melting transition at ~430 °C, instead of the reported temperature of 462 ± 5 °C in literature at ambient pressure [14], and with a slight creeping phenomenon as well.

The melting phenomenon has been very difficult to identify at the beginning due to its unusual foamy appearance. Besides, the total LiOH decomposition does not take place under low pressure despite the same applied temperature protocol since no wide solid state white layer forms contrary to what has been observed under vacuum condition.

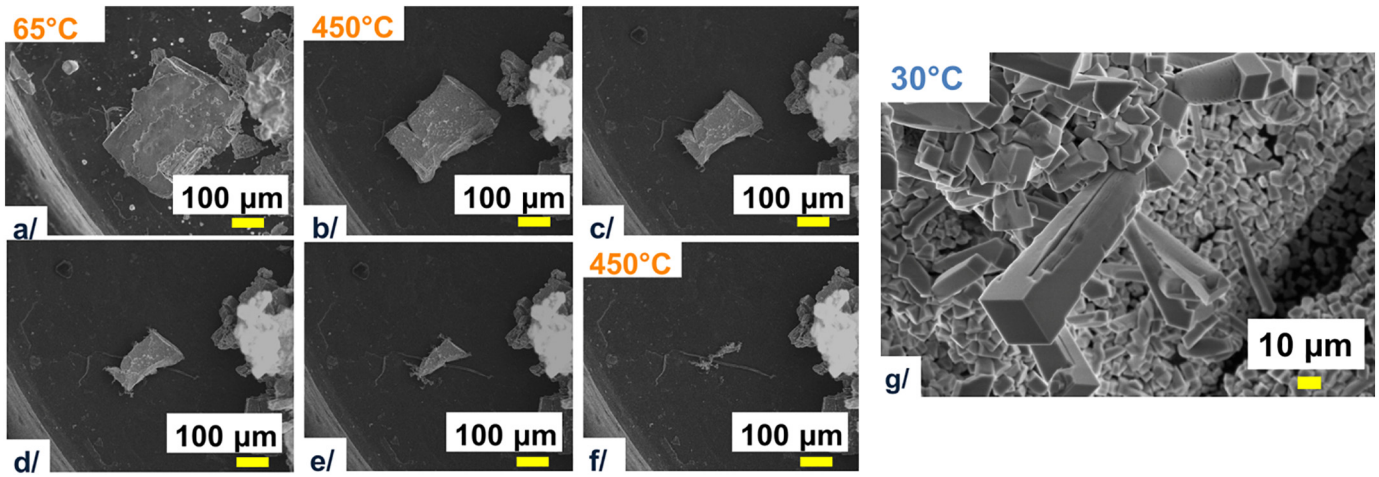

Fig. 6. a/—f/ Highlight on the LiBr grain sublimation at 450 °C and g/related LiBr crystallisation on the edge of the stainless steel protection above the crucible.

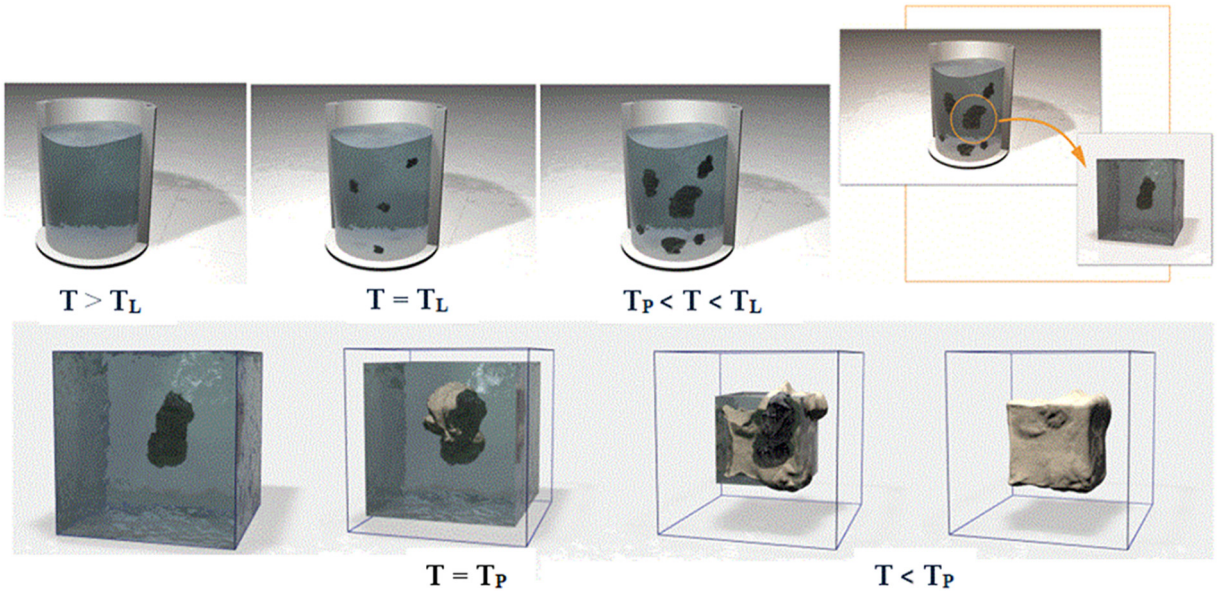

Fig. 7. Theoretical synthesis process of a peritectic compound at ambient pressure during the solidification process under the equilibrium condition.

3.1.3. Characterisations of LiOH after one thermal cycle inside the SEM chamber

The XRD diffractograms confirm that LiOH has been totally decomposed into Li_2O when exposed to vacuum whereas there is a mixture of both Li_2O and LiOH when exposed to the nitrogen-rich environment. According to Myers [23], the LiOH decomposition mechanism, possible only in vacuum or extremely dry environments, begins at 277 °C at the solid/gas interface forming a layer of Li_2O. The water formation at the reaction fronts constitutes the rate-determining step in the conversion of LiOH to Li_2O. Water diffuses then through the formed Li_2O layer up to the solid/gas interface where it is pumped away. This proposed model is in complete agreement with what has been observed in this work, but the phenomenon has been detected around 400 °C instead of 277 °C, confirming rather the observations of [13,24]. Dinh et al. reported that the water release can take place only above 327 °C with a shifting of this value if LiOH undergoes a fast heating [24]. This fact is in well agreement with the DSC results showing that the LiOH decomposition occurs more easily when the heating scanning rate is slow (Fig. 4.). The DSC results show also the same solid-state transition reported by [13] «above which [LiOH] appeared to soften» just before melting, but at 430 °C in our case instead of ~415 °C, and that we

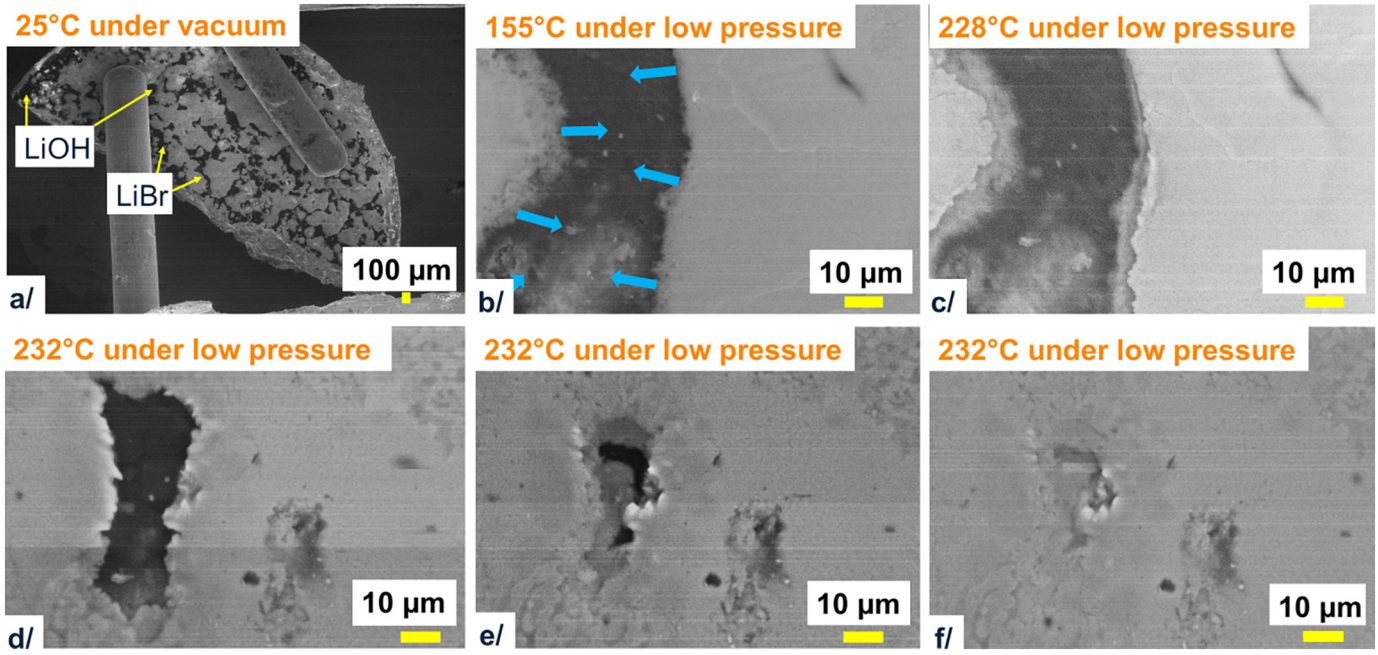

Fig. 8. a/ Pellet of 3LiOH·LiBr where LiBr corresponds to the white areas and LiOH to the dark ones. b/—f/ Zoom in on the LiBr/LiOH/LiBr interfaces and layer-by-layer covering process visualisation (blue arrows).

associate with the LiOH intermediate surface formation above-observed (Fig. 2c/—d/ and 3b/—d/).

As expected, hydrated LiOH does not appear in the XRD diffractogram when the sample under vacuum is not in contact with the ambient atmosphere once out of the SEM chamber. The crucible being not closed, the diffusion of the released water is fostered during the LiOH decomposition towards the chamber's gas, which is itself pumped away preventing the potential reaction reversibility (see supplementary Fig. 3a/). If the sample is briefly in contact with the ambient atmosphere out of the SEM chamber, Li_2O converts into LiOH after a moisture threshold value has been reached. The mixture consists of Li_2O, LiOH and $LiOH \cdot H_2O$ or of Li_2O, LiOH, $LiOH \cdot H_2O$ and Li_2CO_3 (see supplementary Fig. 3b/), as a result of the CO_2 reaction with the sample surface, depending on the time exposure, as demonstrated in [19,20]. The Li_2CO_3 formation has been systematically avoided afterwards.

3.1.4. LiBr under vacuum condition

Regarding LiBr, there is no difference of its behaviour under secondary vacuum or under partial pressure of 10 Pa. The following results are thus presented for the vacuum condition. The phenomena of melting, creeping and of sublimation have been all observed, as seen in Figs. 5 and 6, at a temperature of 464 ± 1 °C instead of a reported temperature of 552 ± 3 °C in literature at ambient pressure. These phenomena explain why the temperature as a function of time is not reliable with the thermocouple in direct contact with the sample at the present time. Another type of crucible is in development to access to this important information.

The temperature gradient allows however clearly identifying the sublimation step from that of the evaporation one. The sublimation phenomenon occurs particularly for the isolated LiBr grains (Fig. 6) at lower temperature (~390 °C) than that also easily observed at the top of the LiBr grains pile. Supplementary video 2 shows an example of the sublimation at secondary vacuum where the LiBr wafers disappear one after one.

Contrary to LiOH, no alteration of LiBr has been noticed, which has been systematically confirmed with the XRD characterisation after each experiment as well with the DSC experiments. Despite a more conventional behaviour than that of LiOH, it is much more difficult to work with LiBr. These results show indeed that this latter has in fact everything to do with the creeping and leakage phenomena observed at macroscale, and not LiOH as commonly believed. These observations allow adjusting the heating scanning rate to optimise the operating conditions. Besides, both the LiOH decomposition and the LiBr grain sublimation are, first of all, surface phenomena. Hence, the pellets are more appropriate to minimise all these effects at micro- and macroscales.

All described behaviours for Alfae Aesar starting materials during the HT-SEM experiments have been also observed with Acros Organics ones.

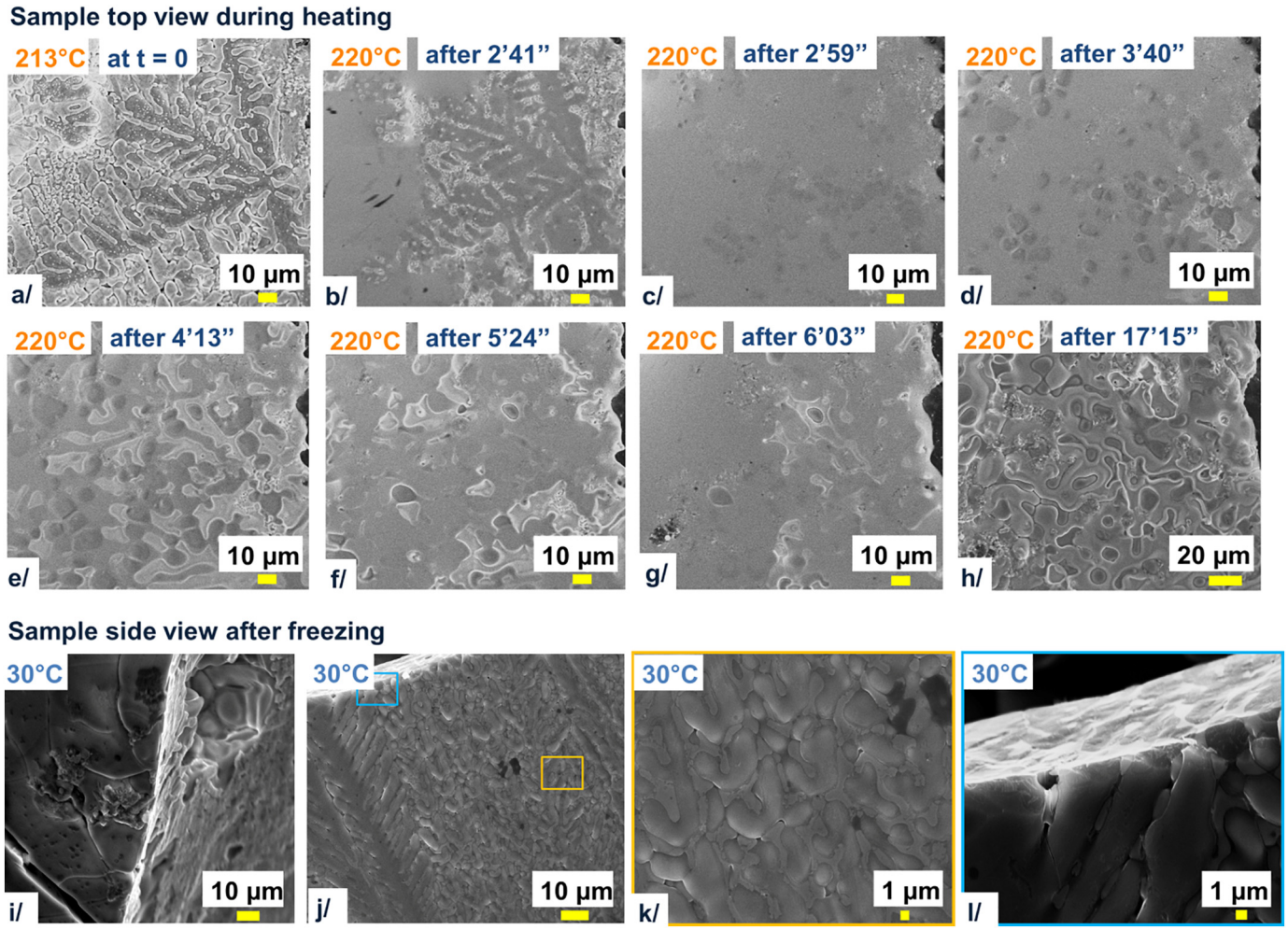

Fig. 9. a/—h/View from the sample top held at 220 °C because of the rapidity of the observed phenomenon: Example of the oscillatory motion effect due to the reaction and infiltration of the LiBr-rich liquid with the LiOH evolving structure once it has been fully covered during the heating step, i/—l/ View from the sample side during another similar experiment fastly cooled up to 30 °C.

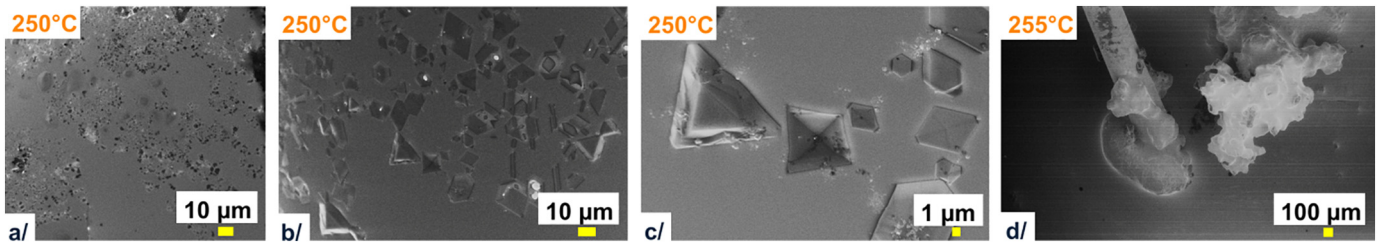

Fig. 10. a/—c/ Occurrence of the LiOH-primary solid phase in the liquid mixture, followed by d/ the dissolution of the LiOH prisms into the liquid mixture.

3.2. The 3LiOH·LiBr mixture theoretical phase transitions

Theoretically and for the best scenario where the equilibrium condition is continuously applied, the solidification of a molten stoichiometric peritectic compound (here, the 3LiOH·LiBr molten mixture) at ambient pressure should start with the formation of a solid primary phase (here, LiOH- primary phase) when the liquidus temperature T_L is reached (380 °C). Then, a reversible and exothermic peritectic reaction takes place at the constant peritectic temperature T_P producing the first solid layers of the stoichiometric peritectic compound at the remaining liquid mixture/ primary phase interface (here, Liquid + LiOH(s) → $Li_4Br(OH)_3$(s) at 304 °C). Once the chemical peritectic reaction ended, the transformation process, related to the atoms diffusion through the solid phases (the remaining LiOH-primary phase and already formed $Li_4Br(OH)_3$), goes on its own up to the temperature reaches the ambient one (Fig. 7.).

This is a real challenge to be able to technically reach and maintain this condition during the experiments, as shown in [3]. Potential locks have to be faced such as a non-congruent solidification (segregation, sedimentation) or/and an incomplete transition, due to the potential sluggish rate of the peritectic transformation, so that the complete transformation would be seldom reached. Yet, $Li_4Br(OH)_3$ has been synthesized with a purity of 99% by using the standard thermal routine but with an enthalpy of ~30% lower than that expected after the first thermal characterisations. By doing this, its morphology remains unknown due to its hardness when extracted from the crucible and the involved mechanisms have remained unattainable [3].

3.3. In situ HT-SEM observation of the 3LiOH·LiBr mixture phase transitions

The results are those obtained under low pressure with Acros Organics raw materials used in [3]. First, LiOH and LiBr are easily distinguishable as shown in Fig. 8a/ and their behaviour is complementary when mixed together, whatever the sample's shape (powder or pellet). During the heating step at 10 Pa, the great affinity of LiBr for LiOH makes it melt and react with the LiOH surface at a lower temperature than the theoretical liquidus one (~230 instead of 304 °C). This reaction takes place layer by layer (Fig. 8b/—f/) supporting the existence of the intermediate surface of LiOH with a distorted lattice up to the fully covering of each LiOH area with LiBr (see subsection 3.1.3 and supplementary video 3).

The LiOH bloating (softening) phenomenon, described in subsections 3.1.1 and 3.1.2, occurs certainly due to a higher temperature under the LiBr covering, facilitating then the infiltration of the LiBr-rich liquid mixture within the increasing porosity of the intermediate surface of LiOH in formation. On the one hand, the presence of LiBr minimises (or even prevents from) the LiOH conversion into Li_2O. On the other hand, this porosity evolution fosters the diffusion and reaction processes inward from the surface layer by layer resulting in an oscillatory motion in the melt not only due thus to the thermal convection (see supplementary video 4). It occurs several times during the melting process, resulting each time in a different morphology (Fig. 9), up to the completion of the reaction between the liquid mixture and the remaining solid LiOH, which at the same time progressively transforms into LiOH metastable intermediate surface. This step explains why a palier time is required and why the use

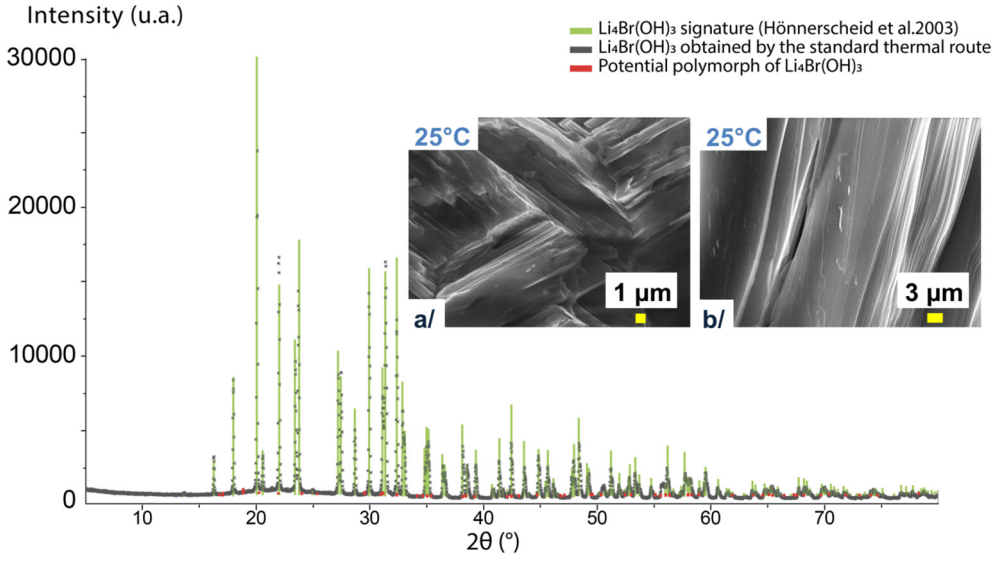

Fig. 11. XRD diffractogram of the 3LiOH ·LiBr mixture after the thermal treatment inside the SEM chamber under low pressure condition confirming the $Li_4Br(OH)_3$ obtention as described by [23] with its related morphology.

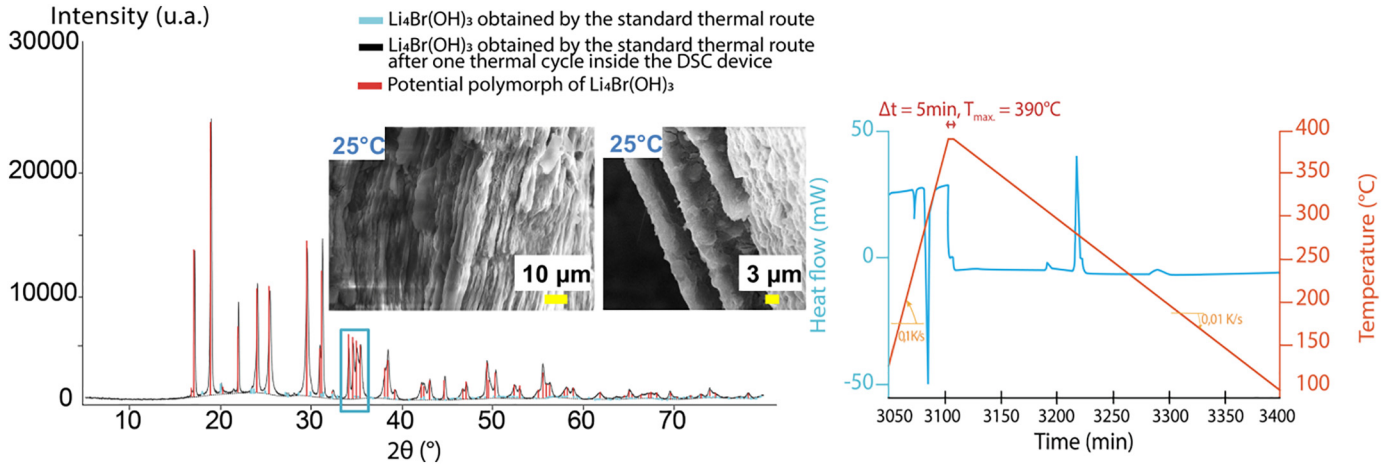

Fig. 12. XRD diffractogram with the related morphology of the potential $Li_4Br(OH)_3$ polymorph obtained with the Alfa Aesar educts. On the right, its related DSC signal.

of a stirring tool is not a mandatory when working at macroscale, except maybe to speed up the mixing, if required.

An oscillatory motion is also mentioned in [6] but for the interaction of liquid mixture flow with solidification processes. In our case, this oscillatory motion occurs during the fusion process. Then, the oscillatory motion stops, the liquid mixture becomes more homogeneous and, very fastly, black solid prisms corresponding to the LiOH-primary solid phase appear around 250 °C. The temperature is then maintained at 255 °C and the remaining liquid mixture reacts with the solid particles up to becoming almost homogeneous (Fig. 10).

So far, the observed transitions are as described by the theory except for the temperature values which are lower than those predicted in theory, as reported also in [15]. For instance, according to the calculated LiOH/LiBr phase diagram, the nucleation of the first LiOH-primary solid phase should have been occurred at the peritectic transition temperature of 304 °C when the temperature increases. All experiments carried out inside the SEM chamber, under vacuum or under low pressure, show a temperature around 250 °C. Then, the LiOH particles should have theoretically been grown and melted completely at the liquidus temperature of 380 °C, changing the final composition of the liquid mixture. The *in situ* experiments show that a temperature gap of 5 °C instead of 76 °C, between the peritectic and liquidus transitions, is sufficient to reach the liquid phase under these applied operating conditions. These observations are also observed with already synthesized $Li_4Br(OH)_3$ submitted to a heat treatment.

As soon as the liquid mixture is almost homogeneous everywhere inside the crucible, the heating step is stopped. A cooling scanning rate of 0.03 °C/s is applied up to 25 °C. The final material is observed first, then characterised by using the XRD powder diffractometer and the DSC device to be compared with that synthesized *ex situ* [3,26].

3.4. Characterisations of the end product synthesized inside the SEM chamber

The XRD results show that $Li_4Br(OH)_3$ has been obtained at 98% as for macroscale experiments [3], confirming definitely its morphology similar with that obtained *ex situ* [26] and consisting of very thin and smooth lamellae (Fig. 11).

2% of minor unknown phase 1 uncharted in the calculated LiOH/LiBr phase diagram is also present. Another experiment consists in synthesizing $Li_4Br(OH)_3$ by following the same protocol but using this time the Alfa Aesar raw materials, which are completely anhydrous contrary to the Acros Organics ones (see subsection 2.1.). The XRD and DSC characterisations (one cycle) show that it corresponds to the previous 2% of unknown phase 1, which is itself the final composition obtained in [3] after the conversion of $Li_4Br(OH)_3$ when its solidification path deviates from the equilibrium condition during the cooling step. Its comprehensive identification by synchrotron radiation and calculations is currently in progress. Meanwhile, the DSC results show a melting temperature very close of 290 °C with a related enthalpy of fusion of ~250 J/g suggesting that this is a potential $Li_4Br(OH)_3$ polymorph that is systematically obtained, and not $Li_4Br(OH)_3$ described by [25]. These results explain now why a deviation of ~30% from the theoretical enthalpy value has been observed in [3] and suggest that this potential $Li_4Br(OH)_3$ polymorph is thermodynamically more stable. This product has besides a lamellar morphology but its slices are much rougher than that of $Li_4Br(OH)_3$. Its related XRD diffractogram is readily recognisable due to its characteristic peak quadruplet at $2\theta = 35°$ (Fig. 12).

These results show also finally that it is not possible to synthesize $Li_4Br(OH)_3$ charted in the current LiOH/LiBr phase diagram with anhydrous raw materials.

The last experiment consists in determining the impact of a total LiOH decomposition into Li_2O on the $Li_4Br(OH)_3$ synthesis process by using directly the $3Li_2O{\cdot}2LiBr$ mixture; LiBr being provided by Acros Organics to be slightly hydrated and thus able to share its hydroxyl groups (see subsection 2.1.). The XRD results show no $Li_4Br(OH)_3$ formation at all but the presence of the peritectoïd compound Li_2BrOH, charted in the LiOH/LiBr phase diagram, Li_2O which does not react completely with LiBr, and another unknown phase 2 already encountered each time LiOH has been, even partially, decomposed in all the previous experiments. This implies that if this new phase 2, also under identification process, is obtained during the synthesis of other products from LiOH and LiBr, then a part of LiOH has certainly been at least partially decomposed into Li_2O.

4. Conclusions and further work

This work follows on from a previous one consisting in developing a new advanced material for thermal energy storage use at high temperature [3]. *De facto*, $Li_4Br(OH)_3$ could be used in ultra-compact storage units contributing thus to a smooth integration, higher penetration levels of renewable energy in hybrid plants and the optimization of the existing standard technologies with a working temperature around 300 °C for instance [27]. A deviation of ~30% from the theoretical enthalpy value of ~800 kJ/kg has however been obtained despite the successful $Li_4Br(OH)_3$ synthesis at macroscale. This study focuses thus specifically on *in situ* and real time experiments at microscale to deepen the understanding of the reaction mechanisms involved in the $Li_4Br(OH)_3$ synthesis process in order to explain the obtained enthalpy deviation of ~30% at macroscale and to alleviate it. The methodology consists

first in monitoring, inside a SEM chamber, the thermally-induced transitions of the starting chemicals LiOH and LiBr. The experimental detection of the LiOH local melting has been unexpectedly difficult even for a very small amount (a few mgs). Besides, the LiOH crystal lattice rearrangement at the solid-state just before melting has been shown as well its decomposition into Li_2O. This latter depends greatly on the presence of water or not in the initial LiOH grain. It has been shown also that if the LiOH decomposition into Li_2O occurs even partially during the $Li_4Br(OH)_3$ synthesis attempt, an unknown phase is formed instead of it (phase under identification process) in addition with a certain amount of Li_2BrOH peritectoïd. Then, these observations allowed unambiguously synthesizing $Li_4Br(OH)_3$ inside the HT-SEM chamber under low pressures. It appears that all transition temperatures of this product is lower than that observed at ambient one. $Li_4Br(OH)_3$ could be hence suggested for storage technologies with a working temperature inferior to 300 °C, which broadens the field of applications. The experiments performed by using the SEM coupled with a hot stage show that the mechanisms occurring at microscale are representative of the ones at the macroscale despite the different working conditions. Hence, this is a powerful tool, saving time and materials, to orientate and determine the right protocols to be used at macroscale. Surprisingly, during this step, two morphologies of $Li_4Br(OH)_3$ have been obtained,-*i.e.* two crystallographic structures with the same chemical formula. One is charted in the current LiOH/LiBr binary phase diagram whereas the other is not. One structure has experimentally a melting temperature of ~288 °C with an enthalpy of fusion of ~250 J/g (the polymorph structure) whereas the other one (charted in the LiOH/LiBr phase diagram) shows a melting temperature of 290 °C with an enthalpy of fusion of ~570 J/g due to a deviation of a part of the composition during the experiment towards another product. This product turns out to be the potential polymorph structure, explaining the observed ~30% loss of enthalpy. The comprehensive identification of the polymorph structure is also currently in progress. Finally, this work demonstrates that $Li_4Br(OH)_3$ charted in the current phase diagram and of interest as a very promising thermal energy storage material cannot be synthesized if LiOH and LiBr are anhydrous or too much hydrated. If however a water amount threshold value is not exceeded, $Li_4Br(OH)_3$ charted in the current phase diagram can be easily synthesized but then, an appropriate temperature protocol has to be applied to avoid its deviation towards another potential more stable polymorph structure of lower enthalpy. These results explain the lost part of enthalpy, definitely related to the moisture-sensitivity of the starting materials LiOH and LiBr. Some current results seem show that it will be possible to obtain the targeted product and to keep it for use. Further experiments to establish reliable temperature curves obtained at microscale during HT-SEM experiments will be performed. The results will be compared with those obtained in reactors inside the standard furnace at macroscale by applying the same operating conditions. This should help to find the appropriate temperature protocol in order to thermally characterise $Li_4Br(OH)_3$ of interest and to study the effects of a thermal cycling.

Supplementary data to this article can be found online at https://doi.org/10.1016/j.matdes.2020.109160.

Data avaibility

The raw/processed data required to reproduce these findings cannot be shared at this time as the data also forms part of an ongoing study (Pc2TES: ANR-16-06–0012CE-01 project).

Credit author statement

Philippe Legros developed and designed the methodology, wrote the Experimental and Results and discussion sections, reviewed the papers, analysed the information, performed the HT-SEM experiments and analysed the results. **Eric Lebraud** performed the DRX experiments, analysed the results and checked the data from literature, **Marie Duquesne** contributed to the discussion of the structure and contents, also improvement of English**, Fouzia Achchaq** conceptualised the research goals and aims, reviewed the papers, wrote the Abstract, Introduction and Conclusions and further work sections, performed the DSC experiments and analysed the results.

Declaration of Competing Interest

The authors declare that they have no known competing financial interests or personal relationships that could have appeared to influence the work reported in this paper.

Acknowledgements

The authors acknowledge financial support from the ANR for subsidizing Pc2TES: ANR-16-CE06-0012-01 project. They also acknowledge Nicolas Penin for his fruitful exchanges and Lucien Céreja (ICMCB), for his valuable assistance in the samples preparation and XRD experiments, as well 25 images communication (https://www.25-images.com/).

References

[1] Y.E. Milian, S. Ushak, L.F. Cabeza, M. Grageda, Advances in the development of latent heat storage materials based on inorganic lithium salts, Sol. Energy Mater. Sol. Cells 208 (2020) 110344.
[2] M. Henriquez, L. Guerreiro, A.G. Fernandez, E. Fuentealba, Lithium nitrate purity influence assessment in ternary molten salts as thermal energy storage material for CSP plants, Renew. Energy 149 (2020) 940–950.
[3] F. Achchaq, E. Palomo del Barrio, E. Lebraud, S. Péchev, J. Toutain, Development of a new LiBr/LiOH-based alloy for thermal energy storage, J. Phys. Chem. Solids 131 (2019) 173–179, https://doi.org/10.1016/j.jpcs.2019.04.001.
[4] H. Kudo, The rates of thermal decomposition of LiOH(s), LiOD(s) and LiOT(s), J. Nucl. Mater. 87 (1979) 185–188.
[5] J. Phillips, J. Tanski, Structure and kinetics of formation and decomposition of corrosion layers formed on lithium compounds exposed to atmospheric gases, Int. Mater. Rev. 50 (2005) 265–286.
[6] W.J. Boettinger, S.R. Coriell, A.L. Greer, A. Karma, W. Kurz, M. Rappaz, R. Trivedi, Solidification microstructures: recent developments, future directions, Acta Mater. 48 (2000) 43–70.
[7] R. Podor, D. Pailhon, J. Ravaux, H.P. Brau, Development of an integrated thermocouple for the accurate sample temperature measurement during high temperature environmental scanning electron microscopy (HT-ESEM) experiments, Microsc. Microanal. 21 (2015) 307–312.
[8] A. Godin, M. Duquesne, E. Palomo del Barrio, J. Morikawa, Analysis of crystal growth kinetics in undercooled melts by infrared thermography, 2014 Conference paper QIRT-2014-104.
[9] M. Duquesne, A. Godin, E. Palomo del Barrio, J. Daranlot Experimental analysis of heterogeneous nucleation in undercooled melts by infrared thermographyby. Conference paper QIRT-2014-076.
[10] T. Liu, M. Long, D. Chen, S. Wu, P. Tang, S. Liu, H. Duan, J. Yang, Investigations of the peritectic reaction and transformation in a hypoperitectic steel: using high-temperature confocal scanning laser microscopy and differential scanning calorimetry, Mater. Charact. 156 (2019) 109870.
[11] R. Podor, J. Ravaux, H.-P. Brau, *In situ* experiments in the scanning electron microscope chamber, in: Viacheslav Kazmiruk (Ed.), Scanning Electron Microscopy, InTech, 2012 , Available from http://www.intechopen.com/books/scanning-electron-microscopy/in-situ-experiments-in-the-scanning-electron-microscope-chamber , ISBN: 978-953-51-0092-8.
[12] R. Podor, G.I. Nkou Bouala, J. Ravaux, J. Lautru, N. Clavier, Working with the ESEM at high temperature-review, Mater. Charact. 15 (2019) 15–26.
[13] R.T. Johnson, R.M. Biefeld, J.D. Keck, Ionic conductivity in Li_5AlO_4 and LiOH, Mater. Res. Bull. 12 (1977) 577–587.
[14] E.P.F. Lee, T.G. Wright, Heats of formation of LiOH ($X^1\Sigma^+$) and $LiOH^+$ ($X^2\Pi$): the ionization energy of LiOH, Chemical Physics Letter 352 (2002) 385–392.
[15] A. Raznoshinskaia, I. Troyanovskaia, V. Kozminykh, Heat-Storing Phase-Change Materials: Influence of Thermophysical Properties on Stabilization of Exhaust Temperature, Materials Today: Proceedings (2019) https://doi.org/10.1016/j.matpr.2019.07.022.
[16] A. Apelblat, A. Tamir, Enthalpy of solution of lithium bromide, lithium bromide monohydrate, and lithium bromide dehydrate, in water at 298.15 K, Journal of Chemistry Thermodynamics 18 (1986) 201–212.
[17] E. Lefebvre, L. Fan, E. Gagnière, S. Bennici, A. Auroux, D. Mangin, Lithium bromide crystallization in water applied to an inter-seasonal heat storage process, Chem. Eng. Sci. 133 (2015) 2–8.
[18] D. Deruto, G. Belleri, L. Barco, V. Longo, Interactions of LiBr with Calcite and Calcium Oxide Powders, 9, 1983 53–58.

[19] S. Li, J. Zhu, Y. Wang, J.W. Howard, X. Lü, Y. Li, R.S. Kumar, L. Lang, L.L. Daemen, Y. Zhao, Reaction mechanism studies towards effective fabrication of lithium-rich anti-perovskites Li3OX (X = Cl, Br), Solid State Ionics 284 (2016) 14–19.
[20] J. Phillips, J. Tanski, Structure and kinetics of formation and decomposition of corrosion layers formed on lithium compounds exposed to atmospheric gases, Int. Mater. Rev. 50 (2005) 265–286.
[21] F. Achchaq, E. Palomo del Barrio, A proposition of peritectic structures as candidates for thermal energy storage, Energy Procedia 139 (2017) 346–351.
[22] H. Kudo, The rates of thermal decomposition of LiOH(s), LiOD(s) and LiOT(s), J. Nucl. Mater. 87 (1979) 185–188.
[23] S.M. Myers, Ion-backscattering study of LiOH-to-Li_2O conversion on a LiH substrate, J. Appl. Phys. 45 (1974) 4320.
[24] L.N. Dinh, W. Mc Lean II, M.A. Schildbach, J.D. Le May, W.J. Siekhaus, M. Balooch, The nature and the effects of the thermal stability of lithium hydroxide, J. Nucl. Mater. 317 (2003) 175–188.
[25] A. Hönnerscheid, J. Nuss, C. Mühle, M. Jansen, The crystal structures of the Lithium hydroxide halides $Li_4(OH)_3Br$ and $Li_4(OH)_3I$, Z. Anor. Allg. Chem. 609 (2003) 317–320.
[26] F. Achchaq, E. Risueño, I. Mahroug, P. Legros, E. Lebraud, B. Karakashov, E. Palomo del Barrio, A. Celzard, V. Fierro, J. Toutain, Development of a carbon felt/salt-based hybrid material for thermal energy storage applications, J. Power Energy 12 (2018) 356–364.
[27] P. Royo, V.J. Ferreira, Z. Ure, S. Gledhill, A.M. Lopez-Sabiron, G. Ferreira, Multiple-criteria decision analysis and characterisation of phase change materials for waste heat recovery at high temperature for sustainable energy-intensive industry, Mater. Des. 186 (2020) 108215.